The Effects of Branching and Deuterium Labeling on Blend Miscibility

Jeffrey DeFelice[a]
[a]Department of Chemistry, Hinman Box 6128,
Dartmouth College, Hanover, NH 03755, USA
jeffrey.j.defelice.gr@dartmouth.edu
Julia S. Higgins[b]
[b]Department of Chemical Engineering and Chemical Technology,
Imperial College, University of London, London SW7 2BY, UK
j.higgins@imperial.ac.uk
Jane E. G. Lipson[a,*]
jane.e.g.lipson@dartmouth.edu

Abstract

The individual and combined effects of 4-arm star branching and deuterium labeling on polystyrene (PS) influence its compatibility in upper critical solution temperature (UCST) and lower critical solution temperature (LCST) mixtures. In this article, we use our Locally Correlated Lattice (LCL) model to characterize a set of PS samples in their pure states in order to predict miscibility trends for blends of PS with poly(vinyl methyl ether) (PVME) (LCST-type mixtures) and isotopic variants of PS (UCST-type mixtures). We find that 4-arm star branching and/or deuterium labeling can shift the pure component properties of PS, such as its percent free volume or cohesive energy density, which affects how the properties of PS 'match' those of the other mixture component. In another section of this article, we turn to modeling the blends, themselves, and provide fundamental thermodynamic insight about the PS/PVME mixtures by calculating the relative enthalpic and entropic contributions to the free energies of mixing. We observe trends in the values of the entropies and enthalpies of mixing for the PS/PVME blends that qualitatively match our pure component properties analysis of the pure PS samples.

Keywords: polymer blend miscibility; free volume; equation of state

1. Introduction

Making a structural [1-24] or chemical [25-36] change to one component of a polymer mixture may cause a notable shift in its compatibility with the other component. In this work, we probe how a structural change (backbone branching) and a chemical change (deuterium labeling) influence the physical properties of polystyrene (PS) in its pure state and its compatibility in mixtures. We analyze experimental data for a set of PS samples for which branching and deuterium labeling were systematically varied. To our knowledge, this report contains the first theoretical study of the combined effects of deuterium labeling and 4-arm star branching on the pure component properties of PS, where these properties were calculated directly from experimental data for the pure state. We find that changes in the physical properties of PS caused by branching and/or deuterium labeling can lead to varying degrees of compatibility upon mixing with another component. The mixtures that we analyze in this work include both upper critical solution temperature (UCST)-type and lower critical solution temperature (LCST)-type blends involving PS, namely, isotopic mixtures of PS and PS/poly(vinyl methyl ether) (PVME) blends, respectively. We find that the relative compatibility of the LCST-type and UCST-type mixtures track with different characteristic pure component properties of the PS samples. We believe that our theoretical study is the first of its kind to consider the combined effects of deuterium labeling and branching in LCST-type blends.

Our approach utilizes information about the pure states to make predictions about their relative compatibilities in a mixture. Using our Locally Correlated Latticle (LCL) theory equation of state (EOS), we have modeled the pressure-volume-temperature (*PVT*) behavior of linear and 4-arm star unlabeled PS (hPS), deuterium labeled linear and 4-arm star PS (dPS), and PVME. The result of this modeling is a set of characteristic parameters that describe each of the pure components, and from which a number of important physical properties can be calculated, e.g. thermal expansion coefficients, % free volumes, and cohesive energy densities (CEDs). Comparing the relative values of these properties leads us to draw conclusions about the relative compatibilities of linear hPS, star hPS, linear dPS, and star dPS, blended with PVME. Following the same approach, we also predict the compatibilities of isotopic PS pairs, e.g. linear hPS paired with linear dPS. Then we model

the PS/PVME blends themselves, using the characteristic molecular parameters we obtained from modeling the pure component experimental data and a single data point for the mixture, the LCST. We explain the shifts in the PS/PVME LCST as a result of branching and/or deuterium labeling on the basis of thermodynamic quantities, in particular, the enthalpic and entropic contributions to the free energies of mixing. We also test the application of a simple averaging approach to predict the LCST of the 4-arm star dPS/PVME blend, which utilizes only information about the other PS/PVME blends.

First, consider only the possible implications of branching on mixed behavior. In cases where the non-bonded mixed interactions between two components are energetically favorable, then increasing the degree to which one component is branched may screen these favorable interactions and thus *reduce* mixture compatibility [5,24,27]. Conversely, if the mixed interactions between components are energetically unfavorable, then increasing the degree to which one component is branched may reduce the number of unfavorable contacts, thus *enhancing* mixture compatibility [3,7,14,22,23]. In addition to the energetic implications of branching on mixing, the effect of branching on the entropy of mixing also plays a role in influencing mixture compatibility. Due to its structure, a branched molecule is more sterically constrained than a chemically identical linear molecule; i.e., a branched molecule has fewer available molecular configurations from which it can sample. For this reason, mixing branched molecules with a linear component may lead to an enrichment of the concentration of branched molecules in the region near the free surface, which reduces their entropic penalty of mixing [37-41]. This physical picture is consistent with experimental surface tension measurements which have indicated that a mixture of branched and linear molecules has a lower surface tension than that of the pure linear melt [38,39,42]. These results highlight the important role of the entropic contribution to the free energy of mixing for branched and linear molecule mixtures. It has been suggested that the effects of branching on the mixture compatibility may be traceable to changes in the properties of the pure state, such as molecular packing efficiency and/or relative free volumes [14,19,43]. Using our Locally Correlated Lattice (LCL) theory equation of state (EOS), we are in a position to test this hypothesis by characterizing and then comparing the pure component physical properties of linear and branched molecules.

Here we examine one type of branched architecture, 4-arm star molecules, and how changing from a linear to a star shaped molecule affects physical properties and mixture compatibility. Star molecules are of particular interest because they can yield unique and sometimes more useful macroscopic properties than a material comprised of chemically identical linear molecules. Some examples include: the addition of star molecules into a polymer blend [1,14] or nanocomposite, [21] which can improve mixture compatibility and/or desirable mechanical properties. Also, star shaped molecules have been found to be particularly useful in biomedical applications, as highlighted in a recent review by Wu et al. [44].

There are two fundamental characteristics of star molecules that influence their physical properties: the *number* of star arms and the *molecular weight* (MW) of each arm. Here we provide a brief overview of how changes in the number of star arms and/or the MW of each arm may affect a number of macroscopic properties. First, consider star molecules which are comprised of low MW arms. In this case, there are a number of reports in the literature [45-55] that the behavior of a star molecule may notably differ from that of a chemically identical linear molecule whose MW roughly matches that of each star arm. For example, surface tension measurements reported by Qian and coworkers [39] showed that (MW = 7,000 g/mol) 4-arm and 11-arm star polystyrene (PS) melts have lower surface tensions than that of a linear PS melt. For the 11-arm star PS melt, the surface tension was lower than that of linear PS by 15% [39]. In other recent work, McKenna and coworkers [42] reported that the surfaces of glassy 3-arm and 8-arm star PS samples were more compliant than that of their linear analog.

Other differences between the properties of low MW star molecules and linear molecules that have been observed include: molecular packing [45,46] and the glass transition temperature (T_g) [45,46,49,56]. Molecular dynamics (MD) simulations performed by Chremos and coworkers [45] indicated that the number bead density increases by ~10% from a linear chain to a 12-arm star molecule, when the number of beads comprising an arm matched that of the linear chain, and was equal to 5. Turning to

the glass transition, simulations [45,46] and experimental measurements [49] show that for low molecular weight species, the *bulk* T_g decreases as the number of arms increases; i.e. from a linear molecule to one with many arms. In nanometrically thin *films*, however, Glynos and coworkers [49] have recently reported that low molecular weight star molecule films may exhibit a range of thickness-dependent T_g behavior, which is determined by the number of star arms. For example, as the thickness of a 3-arm star PS (arm MW = 10,000 g/mol) film decreased below 100 nm, its T_g was *suppressed* from that of the bulk value [49]. The thickness-dependent T_g behavior observed for the 3-arm star PS film, is consistent with that reported for linear PS films [49]. In contrast, as the thickness of a 16-arm star PS (arm MW = 10,000 g/mol) film decreased below 100 nm, it exhibited T_g *enhancement* relative to the bulk value [49].

In contrast to the results for low MW star molecules described above, there is some evidence that suggests that the physical properties of star molecules converge with those of their linear analog as the MW of each arm increases. Chremos and coworkers [45] found that the number bead densities and bulk T_g values of 3 through 16 arm star molecules approach that of their linear counterpart as the length of the star arms reach ~40 beads. Experimental bulk T_g measurements reported by Glynos and coworkers [49] also show that increasing the MW of each arm brings the star T_g closer in value to that of the linear species. Further, the thickness-dependent T_g behavior of films also converges between star and linear molecules as the star arm MW increases [49].

In cases such as these, where the physical properties of high MW star and linear molecules are similar in the pure state, one might expect that their behavior in the mixed state would also be comparable. Experimental results for linear and star PS blends with poly(vinyl methyl ether) (PVME) support this conclusion. Pavawongsak et al. [12] reported that the cloud point temperatures of linear PS (MW = 275,000 g/mol) blended with PVME (MW = 99,000 g/mol) was only 3 °C greater than that of a 3-arm star PS (MW = 255,000 g/mol) sample blended with the PVME. In other work, Sremcich et al. [15] performed cloud point measurements on higher functionality star PS samples, including 14, 18, and 22-arm star PS (MWs ranging from roughly 500,000 – 1,000,000 g/mol) blended

with PVME (MW = 99,000 g/mol), as well as the analogous linear PS/PVME blends for comparison. From their measurements, Sremcich and coworkers [15] concluded that there was no observable difference between the miscibility of a high MW linear PS/PVME blend and a star PS/PVME blend. Taken together, the results of both studies suggest that branching has a negligible effect on the miscibility of PS/PVME blends when the MW of PS is approximately greater than 200,000 g/mol.

In addition to branching, a chemical change (e.g., isotopic labeling) may also influence mixture compatibility. This is particularly relevant for Small Angle Neutron Scattering (SANS) studies. SANS is an experimental technique that is able to characterize the compatibility of a mixture; it requires that one component be deuterium labeled. The zero angle scattering intensity collected as a function of temperature from SANS measurements is directly related to the second derivative of the free energy of mixing as a function of composition, $\left(\partial^2 \Delta G_{mix}/\partial \phi^2\right)_{T,P}$ [32]. These data are often interpreted in terms of the Flory-Huggins χ parameter, for example, an increase (decrease) in the value of χ upon physically or chemically changing one component of the mixture is taken to mean that there are more unfavorable (favorable) non-bonded interactions between the components [57]. One critical limitation of Flory-Huggins solution theory, and thus a χ parameter-based analysis, is that it cannot predict LCST-type phase separation [57]. Another potential limitation is that in some cases, $\chi(T)$ for a mixture has been interpreted in order to provide insight about the compatibility of the *unlabeled* blend components. However, experimental cloud point measurements have shown that deuterium labeling can notably shift blend miscibility [25-36]. Therefore, an interpretation of χ for the mixture may not always reliably reflect pure component behavior. For example, the lower critical solution temperature (LCST) of an unlabeled linear PS (hPS)/PVME blend is shifted upward by ~40 K as a result of deuterium labeling the PS component (dPS) [32,35,36]. Therefore, measurements performed on the labeled PS/PVME blend do not provide clear insight about the compatibility of the unlabeled blend. Previous work by White et al. [32] using the LCL theory illustrated that the change in PS/PVME miscibility upon deuterium labeling is caused by changes in the pure component properties from hPS to dPS,

specifically, the thermal expansion coefficient and % free volume, which leads to different degrees of compatibility with PVME.

In a study by Graessley and coworkers, [27] a set of polybutadiene (PB) homopolymer blends were characterized via SANS measurements and it was observed that the value of χ increased when the more branched PB component was deuterium labeled versus when the less branched component was labeled. These results led Graessley and coworkers to propose that deuterium labeling and branching may have opposite, or competing, effects on the strength of the intermolecular interactions [27]. Other results, such as those reported by Greenberg et al. [5,6] for PS homopolymer blends, are consistent with behavior of the PB blends described above; i.e., χ is more unfavorable (increases) when the more branched component is deuterium labeled. For example, Greenberg and coworkers observed that χ is greater for a 4-arm star dPS/linear hPS blend than that of a linear dPS/linear hPS blend [5].

One of the goals of this work to use the LCL theory to predict the compatibility of isotopic pairs of linear and 4-arm star PS based only on their pure component properties, and make connections with the experimental trends for the mixtures. The paper is organized as follows. In section 2, we provide background information on the LCL theory and describe its implementation for modeling pure components and mixtures. We also provide the LCL model definitions for CED and % free volume in this section. In section 3.1, we report and discuss our results from modeling the pure component experimental *PVT* data using the LCL EOS and compare the effects of branching, of deuterium labeling, and the combined effects of both branching and deuterium labeling on the pure component properties of PS. In section 3.2, we predict how the pure component properties, alone, may influence the compatibility of LCST-type PS/PVME blends. We turn to UCST-type mixtures in section 3.3 and apply the same analyses of pure component properties to rank the compatibility of PS isotopic pairs. In section 4.1, we shift from analyzing pure component data, alone, and apply our LCL model to the set of PS/PVME blends in order to study the effect of branching and deuterium labeling on the LCST value. We examine the underlying effects of branching and deuterium labeling on blend miscibility in more

detail in section 4.2 by calculating and comparing the enthalpic and entropic contributions to the free energies of mixing. In section 5, we summarize our findings and conclusions.

2. Theory and Implementation

2.1. Model Equations and Molecular Parameters

This section provides a brief explanation of our theory, the Locally Correlated Lattice (LCL) model, which is used to model the polymer melts and blends. Our LCL model has been previously applied to a variety of polymer melts, solutions and blends, [32,58-63] as well as small molecule fluids and mixtures [64,65]. While we provide in this section an overview of the fundamentals we do not give detailed derivations, as those may be found in numerous earlier studies [58,63-66].

Our theoretical treatment is a lattice-based model for chain fluids that incorporates the effects of free volume (i.e. compressibility) and naturally accounts for the effects of nonrandom mixing. A temperature dependent expression for the internal energy ($U(T)$) is obtained using results derived (via integral equation methods) [66] for the temperature dependent nearest neighbor segment-segment conditional probabilities; thus incorporating "local correlations" as opposed to being solely mean field-based. Making use of the Gibbs-Helmholtz relationship ($U(T) = \mathrm{d}(A/T)/\mathrm{d}(1/T))_{Ni,Nj,V}$) and integrating $U(T)$ from an athermal reference state (using Guggenheim's result [67]), the expression for the Helmholtz free energy (A) is derived. Once we have derived an analytical expression for the free energy, all other thermodynamic quantities of interest can be obtained. The Helmholtz free energy for a binary mixture of molecules types i and j is given by:

$$\begin{aligned}\frac{A}{k_B T} = {} & N_i \ln \phi_i + N_j \ln \phi_j + N_h \ln \phi_h \\ & + \frac{N_i q_i z}{2} \ln\left(\frac{\xi_i}{\phi_i}\right) + \frac{N_j q_j z}{2} \ln\left(\frac{\xi_j}{\phi_j}\right) + \frac{N_h z}{2} \ln\left(\frac{\xi_h}{\phi_h}\right) \\ & - \frac{N_i q_i z}{2} \ln\left[\xi_i \exp\left(\frac{-\varepsilon_{ii}}{k_B T}\right) + \xi_j \exp\left(\frac{-\varepsilon_{ij}}{k_B T}\right) + \xi_h\right] \end{aligned} \quad (1)$$

$$-\frac{N_j q_j z}{2}\ln\left[\xi_i \exp\left(\frac{-\varepsilon_{ij}}{k_B T}\right)+\xi_j \exp\left(\frac{-\varepsilon_{jj}}{k_B T}\right)+\xi_h\right]$$

where:

$$N_h = \left(\frac{V}{v}\right) - N_i r_i - N_j r_j$$

$$\phi_\alpha = \frac{N_\alpha r_\alpha}{N_i r_i + N_j r_j + N_h} = \frac{N_\alpha r_\alpha v}{V}$$

$$\xi_\alpha = \frac{N_\alpha q_\alpha}{N_i q_i + N_j q_j + N_h}$$

$$q_\alpha = r_\alpha z - 2r_\alpha + 2$$

A is expressed as a function of the independent variables N_i, N_j, V, and T, which are, respectively: the numbers of molecules of components i and j, the total volume of the mixture, and the absolute temperature. We work on the simple cubic lattice, thus the lattice coordination number, z, is fixed at $z = 6$; k_B is the Boltzmann constant. Each component is described by three model parameters: r_i (r_j) - the number of segments per molecule of type i (j), v - the volume per lattice site, and ε_{ii} (ε_{jj}) - the non-bonded segment-segment interaction energy between nearest-neighbor segments of types i-i (j-j). For mixtures, an additional parameter, ε_{ij}, that characterizes the interaction between nearest-neighbor segments of type i and j is needed, and is discussed further below. N_h represents the total number of unoccupied lattice sites (h stands for "holes"); this value is fixed by minimizing the system's Gibbs free energy ($G = U - TS + PV$) at a given composition and set of $\{T, P\}$ conditions, which determines the free volume. The total volume, V, is then the sum of the hard core volume of the molecules, $N_i r_i v + N_j r_j v$, and the free volume $N_h v$. The remaining definitions in equation 1 are as follows: ϕ_i is the volume fraction of sites of type i; ξ_i is a concentration variable that defines the fraction of non-bonded contacts ascribed to component i out of the total number of non-bonded contacts in the system, where, due to local connectivity, a molecule of type i has $q_i z$ non-bonded contacts.

Recall that each component of the mixture is described by its three pure component model parameters r, v, and ε (note that in the following discussion, we have dropped the i or j subscript because we are discussing a component in the pure state). Here we introduce

the route through which we characterize the pure component parameters, which is via the equation of state (EOS) derived from our LCL theory, given by:

$$P = -\left(\frac{\partial A}{\partial V}\right)_{N,T} = \left(\frac{k_B T}{v}\right)\ln\left(\frac{1}{\phi_h}\right) + \left(\frac{k_B T z}{2v}\right)\ln\left(\frac{\phi_h}{\xi_h}\right) - \left(\frac{k_B T z \xi}{2v}\right)\left(\frac{\xi\exp[-\varepsilon/k_B T] - 1}{\xi\exp[-\varepsilon/k_B T] + \xi_h}\right) \quad (2)$$

The expression for the EOS shown in equation 2 follows from the thermodynamic relationship ($P = -(\partial A/\partial V)_{N,T}$ where the Helmholtz free energy, A, is that of a single pure component. Note that although P is expressed in terms of the independent variable V in equation 2, V cannot be directly expressed as a function of P (as is typical with many theoretical EOS's). Therefore, in applying the model, we use numerical root finding to determine V in situations where P is the known input variable.

In addition to the result for the EOS, the Helmholtz free energy given in equation 1 leads to analytic expressions for the other thermodynamic properties of the mixture, including the internal energy ($U = (\partial(A/T)/\partial(1/T))_{Ni,Nj,V}$) and entropy ($S = -(\partial A/\partial T)_{Ni,Nj,V}$). It is often more convenient to define these functions in terms of intensive variables. For example, the set of independent variables [N_i, N_j, V, T] can be reduced to the set [x, $\overline{V}$, T] where x is the mole fraction of component i, $\overline{V} = V/N$ is the intensive volume per molecule, and $N = N_i + N_j$ is the total number of molecules. Correspondingly, one then calculates the intensive properties: $\overline{A} = A/N$, $\overline{S} = S/N$, etc. In this work, we define the intensive variables in a "per mass" basis, which is more convenient for polymers due to their high MW. In this case, the over-bar notation signifies any quantity per total mass, and the composition variable x is thus the mass fraction.

2.2. Model Implementation

The fit of the EOS (equation 2) to experimental *PVT* data is optimized in order to determine values for the parameters r, v, and ε for each of the pure components. It is important that we fit over a consistent temperature and pressure range for all of the pure

components of interest in order to compare properties between different samples. As is true for other equation of state approaches, the best-fit parameters for the LCL theory also vary with respect to the midpoint of the fitting range, which is caused by the overly strong temperature dependence of the thermal expansion coefficient [60,61]. Therefore, by characterizing all of the samples over the same fitting ranges, we eliminate the influence of the temperature dependence on the best-fit parameters and can most accurately compare different samples relative to one another. In this work, we used a *T*-range of 383 – 475 K and a pressure range of 0 – 100 MPa to maintain internal consistency for all of our samples.

In some cases, we may be limited by the unavailability of *PVT* data for a particular MW polymer sample. However, if *PVT* data are available for a *different* MW of the same polymer species, we can model it with the MW of interest because r scales linearly with MW, such that: $r_{new} = MW_{new}(r_{old}/MW_{old})$, which keeps the quantity r/MW constant and without changing v or ε. Although each pure component has three characteristic parameters, we describe mixtures using a single v throughout, such that all components fit the same lattice. The mixture v is a "compromise" value, e.g. the arithmetic mean of the pure component v values, which best maintains the model agreement with the experimental pure component *PVT* behavior. While we change v to model the mixture, the hard core volume, rv, obtained from the pure component modeling is kept constant, i.e. the r parameter is adjusted to account for the change in v such that: $r_{new}v_{new} = r_{old}v_{old}$ (note that ε remains unchanged).

In order to work with mixtures we require a value for the interaction energy, ε_{ij}, between non-bonded segments of type i and j. This mixed interaction parameter can be expressed as the geometric mean of the pure component parameters ε_{ii} and ε_{jj} scaled by a factor g.

$$\varepsilon_{ij} = g\left(\varepsilon_{ii}\varepsilon_{jj}\right)^{1/2} \tag{3}$$

Just as pure component experimental *PVT* data are used to obtain values for r, v, and ε, some information about the mixture must be known in order to quantify ε_{ij}, or equivalently, g. Examples include: a lower or upper critical solution temperature [58-61] or small angle neutron scattering data [32] (where, as noted above, the zero angle scattering intensity as a function of temperature is related to the second derivative of the free energy with respect to composition). In this work, experimental LCSTs were available in the literature for the linear and 4-arm star hPS/PVME blends, and the linear dPS/PVME blend. Using these data, the g-value for each blend was set such that it yielded the experimental blend LCST.

The mixed interaction energy and pure component parameters may then be used to model the mixture behavior and calculate the associated changes in thermodynamic quantities upon mixing. Of course, the Gibbs free energy of mixing (ΔG_{mix}) is required in order to predict the spinodal and/or binodal phase boundary, however, knowledge regarding the separate entropic (ΔS_{mix}) and enthalpic (ΔH_{mix}) contributions can also be very revealing. A theoretical route to these quantities is valuable, as they are typically not available experimentally. Here it is important to demonstrate that such predictions are likely to yield real physical insight; there are numerous theoretical examples in which cancellation of errors in the contributions to ΔG_{mix} work to produce a reasonable estimate of the overall sum, but not of its parts. In previous studies we have tested the ability of our model in this area by showing that our predictions for the thermodynamic contributions to mixing compare well with experimental values determined via SANS data for a deuterium labeled polystyrene/poly(vinyl methyl ether) blend [32] and ΔH_{mix} data for a polystyrene/polybutadiene blend [58]. We therefore include analogous results for the mixtures of interest here in the work we discuss below.

2.3. Cohesive Energy Density and Free Volume

Two quantities that will prove illustrative in our analysis are ones that cannot be experimentally measured for polymers: the cohesive energy density (CED) and the Free Volume (FV; we will actually be interested in %FV values). For small molecules, the CED is defined as the energy of vaporization per unit volume of fluid. Experimentally, the CED can be calculated from enthalpy of vaporization measurements. However, polymeric

species are non-volatile, and in these circumstances a theoretical route to U (and therefore the CED) is useful [because an analogous theoretical definition for the CED is the absolute value of the internal energy divided by the volume, $|U|/V$].

We predict CED values for our polymers of interest by applying the analytical result for U, which is derived using our LCL theory via the thermodynamic relationship $U = (\partial(A/T)/\partial(1/T))_{Ni,Nj,V}$. This is given below:

$$U = \left(\frac{\partial(A/T)}{\partial(1/T)}\right)_{N,V} = \left(\frac{Nqz}{2}\right)\left[\frac{\varepsilon\xi\exp[-\varepsilon/k_BT]}{\xi\exp[-\varepsilon/k_BT] + \xi_h}\right] \quad (4)$$

We have found that CED values can be useful as a guide to miscibility under certain circumstances [60,63]. However, its application in the literature has been extensive, mainly through its relationship to the solubility parameter, δ, which is defined as the square root of the CED, $\delta = (|U|/V)^{1/2}$. There is a history in the literature of taking the difference between δ values of two species to generate an approximation for the energy change upon mixing, $\Delta U_{mix} \propto (\delta_i - \delta_j)^{1/2}$, which is then used to try and predict the mixture behavior. Note that this approach will always lead to $\Delta U_{mix} > 0$ and thus does not predict an LCST [57]. This strategy has had very limited success, mainly for some classes of small molecule mixtures; its success for polymer mixtures has largely been restricted to some of the polyolefin blends, as reported by Graessley and coworkers [68,69]. Even in that set, though, the solubility parameter approach fails to predict the LCST-type behavior observed experimentally for polyolefin blends containing poly(isobutylene) (PIB) [69]. Instead, it predicts the UCST-type behavior common to the other polyolefin blends. In a previously-published analysis of these systems we explain the result by showing that while the CED of PIB lies well within the range occupied by the set of polyolefins, its % free volume (defined just below) makes it an outlier in this group [60,63]. We therefore ascribe the 'irregular' phase behavior to a mismatch in % free volume, noting that this quantity is truly distinct relative to the CED.

Turning to free volume, recall that in our model the total volume (V) at a chosen T and P is the sum of the hard core volume and free volume: $V = Nrv + N_h v$. Thus the model definition of the free volume is: FV = V - Nrv, and it accounts for the portion of the total lattice volume that is made up of unoccupied sites. We have shown that the percent free volume predicted by the LCL theory to be present in a polymer species is correlated with the magnitude of its thermal expansion coefficient, however, it is not correlated with CED. Therefore, free volume and CED are properties that may both serve as useful metrics for predicting mixture behavior, depending on the situation.

As mentioned above, it is necessary to characterize all components over the same temperature and pressure ranges in order to reasonably compare their properties, such as %FV and CED. Further, these properties should always be calculated for the same temperature and pressure when making comparisons between different samples. Maintaining an internally consistent application of the LCL theory is important because choosing a different temperature or pressure can have a significant effect on %FV, while a change in the lattice size will impact the value of the CED [60]. In the former case, the change in %FV with temperature (pressure) can be traced to the thermal expansion (compressibility) of the sample. Therefore, the %FV values reported in this work were all calculated at the same temperature and pressure (400 K and 1 atm) for each sample. In the latter case, the lattice size (v) affects the CED because it controls the number of segments per overall volume, and thus is related to the available surface area for intermolecular interactions. Because the v parameter is obtained by the LCL theory EOS fit to experimental PVT data, the influence of the v value on the CED underlines the importance of characterizing all samples over the same temperature and pressure ranges.

3. Pure Component Analysis

3.1. Analysis of Pure PS: Effects of Branching and Deuterium Labeling

We begin our analysis with a comparison of the pure component properties calculated for the PS samples and PVME. We modeled the PVT behavior of linear hPS (MW= 460,000 g/mol), 4-arm star hPS (MW= 520,000 g/mol), linear dPS (MW= 114,000

g/mol), 4-arm star dPS (MW= 400,000 g/mol), [70] and PVME (MW= 99,000 g/mol), [71] using our LCL theory EOS (equation 2); the results corresponding to the atmospheric pressure isobars are shown in Figure 1. The characteristic model parameters obtained from the EOS modeling are tabulated in Table 1.

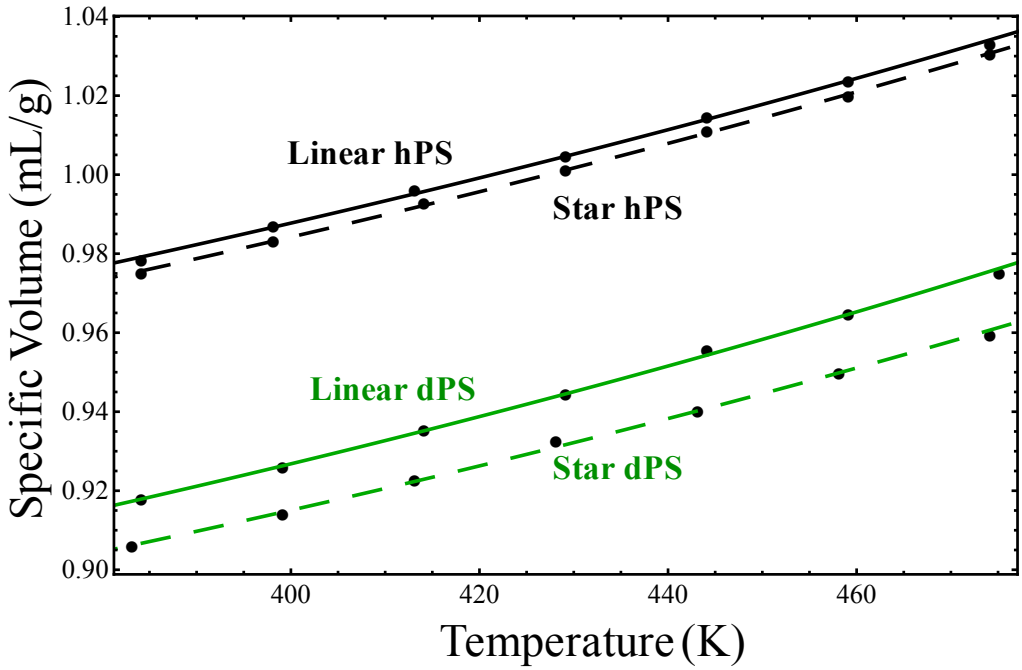

Figure 1. LCL EOS model fits (curves) to the experimental data (points) [70] for 1 atm isobars of the linear and star polymers.

	MW (g/mol)	*r*	*v* (mL/mol)	*r*/MW $(g/mol)^{-1}$	$\lvert \varepsilon \rvert$ (J/mol)	α ($x10^{-4}$ K^{-1})	%FV	CED ($\lvert E \rvert / V$) (J/mL)
Linear hPS	460,000	37360.0	10.7074	0.0812174	2174.7	5.60	11.9	323
Star hPS	520,000	43407.3	10.3736	0.0834756	2168.3	5.63	12.0	331
Linear dPS	114,000	10752.3	8.5480	0.0943184	2067.0	6.22	13.0	376
Star dPS	400,000	37790.7	8.4750	0.0944768	2117.2	5.92	12.5	393
PVME	99,000	10633.0	8.2893	0.107404	1998.9	6.69	13.8	368

Table 1. Characteristic model parameters obtained from LCL EOS model fitting and calculated physical properties of the pure components.

The experimental *PVT* data for linear hPS (MW = 460,000 g/mol) and star hPS (520,000 g/mol) shown in Figure 1 illustrate that 4-arm branching has a limited effect on the

macroscopic behavior of high MW PS. Note that for these samples, the total MWs of the linear and star hPS samples are comparable and relatively large, thus we would expect that their *PVT* behavior would not significantly differ, for the reasons outlined in section 1. The model parameters for linear and star hPS listed in Table 1 also reflect the similarities between samples. For example, we find that this degree of branching has a negligible effect on $|\varepsilon|$, which decreases by only 6.4 J/mol from linear to star hPS. In previous work characterizing a large number of polymeric systems White and Lipson have shown that $|\varepsilon|$ values are strongly correlated to the thermal expansion coefficient ($\alpha = (1/V)(\mathrm{d}V/\mathrm{d}T)_P$) [60,63]. One can visually observe from Figure 1 that the slopes of the LCL EOS model fits to the experimental *PVT* data, $(\mathrm{d}V/\mathrm{d}T)_P$, for linear and star hPS are roughly parallel. Further, our calculations of the α values for linear and star hPS listed in Table 1, which are 5.60 and 5.63 ($\times 10^{-4}$ K^{-1}), respectively, indicate that branching also has a negligible effect on the thermal expansion of hPS. Our conclusion is consistent with experimental measurements by Simon et al., which indicated essentially no difference between the α values for linear and 3-arm star hPS samples [72].

Turning to the effect of deuterium labeling, the experimental *PVT* data shown in Figure 1 illustrate that deuterium labeling produces a notable shift in the specific volume, $V(T)$, over this temperature range: linear dPS has a much smaller *specific* volume (in units of mL/g) than linear hPS. The LCL model parameters listed in Table 1 also reflect the observable difference in the *PVT* data, indicating that deuterium labeling increases the number of theoretical segments per mass (r/MW) and notably weakens intermolecular interactions ($|\varepsilon|$) relative to linear hPS. The reduction in $|\varepsilon|$ caused by deuterium labeling yields an increase in the thermal expansion coefficient (α) compared to that of linear hPS, which can affect its mixture compatibility [32,61]. One factor that influences this shift in $V(T)$ is the exchange of hydrogen atoms for heavier deuterium atoms, which increases the mass per segment. To account for the effect of deuterium labeling on the mass per segment of PS, White and Lipson [32] compared the volumes of linear hPS and linear dPS *per mole of repeat units*, finding that the shift in the *PVT* behavior of PS upon deuterium labeling cannot simply be explained by the change in mass per segment. They found that linear dPS has a larger volume per mole of repeat units than linear hPS, [32] and the data shown

in Figure 1 are consistent with their findings when compared on this basis. In addition to increasing the mass per segment, a deuterium labeled C-D bond is shorter than an unlabeled C-H bond, which may reduce the hard core volume of PS [73]. However, a reduction in bond length also reduces polarizability, thus weakening the intermolecular interactions and increasing the hard core volume [73]. These competing effects of deuterium labeling may be further complicated by molecular architecture, i.e. in the case of star dPS, which we will discuss below.

While previous reports have covered the independent effects of star topology [6,11,12,15,16,24] and deuterium labeling [25,26,32,35,36,61] in comparison to linear hPS, here we present the first results which reflect the combined effects of branching *and* deuterium labeling. A distinct shift in the experimental *PVT* data is evident, and is shown in Figure 1. These data indicate a larger shift in the specific volume as a result of deuterium labeling star PS than by deuterium labeling linear PS. Note that for linear and star dPS, the MW of each star dPS arm is closer to that of the total MW of linear dPS. However, the star dPS arm MW and total MW of the linear dPS are sufficiently large such that these samples may be compared fairly, as outlined in section 1. Subsequently, the difference in *PVT* behavior between linear and star dPS is also reflected in the LCL model parameters listed in Table 1. In particular, we find that *rv*/MW is *slightly more* reduced and that $|\varepsilon|$ is *less* strongly reduced upon deuterium labeling star PS than by deuterium labeling linear PS. Further, we predict a 50.2 J/mol increase in $|\varepsilon|$ going from linear to star dPS, and calculate a ~5% difference in their α values. Therefore, both the experimental *PVT* data and our theoretical calculations indicate that the strength of the effect of deuterium labeling on pure component properties is not the same for linear and star architectures of PS. One possible physical interpretation of our results is that some of the weakening effect caused by deuterium labeling on the interaction strength is mitigated by the close proximity of segments near the star core of star dPS.

3.2. Comparisons of Pure PS Samples with PVME

Because we are interested in the blends of the PS samples with PVME, we will compare how their pure component properties 'match' or 'mismatch' with those of PVME.

Most recently, we have noted that some miscibility trends for LCST-type systems correlate with our LCL predictions for percent free volume (%FV), [60,62,63] the calculation of which was described in the previous section. Mismatches between pure component %FV values are associated with the strength of the entropic penalty of mixing, thus they track well with LCST-type miscibility trends. We have also found that %FV is inversely correlated with both $|\varepsilon|$ and α, i.e. % free volume *increases* as $|\varepsilon|$ and α *decrease* [60,63]. Therefore, %FV, $|\varepsilon|$, and α together, provide insight about the relative miscibility of LCST-type mixtures. In Figure 2, we illustrate the relationship between the percent free volumes %FVs (calculated for all species at 400 K and 1 atm) and $|\varepsilon|$ for the set of PS samples and PVME.

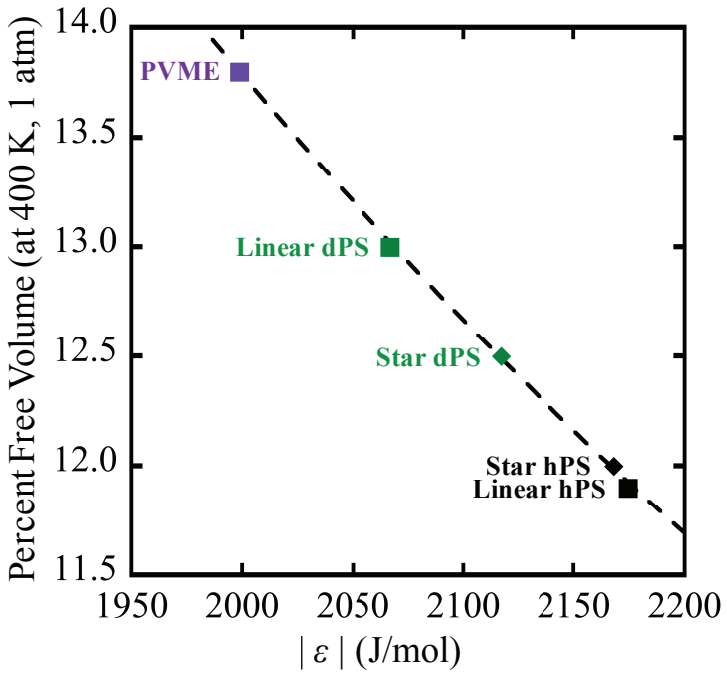

Figure 2. Correlation between %FV and $|\varepsilon|$. All % free volumes were calculated for $T = 400$ K and $P = 1$ atm. Dashed line serves as guide to the reader's eye.

The closest %FV match with PVME (at 13.8%) is linear dPS (at 13.0%), which suggests that PVME/linear-dPS would be the most compatible blend, according to this criterion. Next, is is star dPS, for which we calculate a %FV of 12.5%, followed by linear and star hPS, which have 11.9%FV and 12.0%FV, respectively. We would therefore predict that linear and star hPS are essentially equivalent and the least miscible with PVME, within this

comparison group. This trend also allows us to draw some conclusions regarding the individual and combined effects of branching and deuterium labeling on %FV, and these are discussed below.

First consider the effect of branching on the hPS samples, where we find that going from linear to star hPS yields a negligible increase in %FV of about 0.1%. Simulations of chemically identical linear and branched polymers in their melt state, such as the work of Chremos and Douglas, [45] and others, [46-55] indicate that the segment density of a low functionality star (e.g., fewer than 6 arms) approaches that of a linear chain, as the arm molecular weight increases. Their results suggest that the free volume of a high molecular weight linear polymer and a low functionality, high molecular weight star polymer should be roughly equivalent. The %FVs that we calculated for linear and star hPS support this hypothesis.

We find the greatest impact on %FV to be when linear PS is deuterium labeled, where the percent free volume increases by about 1.1% from linear hPS to linear dPS. It is important to verify that the difference in the MWs of the linear hPS and linear dPS samples that we are comparing is not the underlying factor responsible for their differences in %FV or the other pure component properties. In previous work, White and Lipson [60] characterized a MW = 110,000 g/mol linear hPS sample using the LCL model over nearly the same T and P ranges as the MW = 460,000 g/mol linear hPS sample used in this work. The MW of that 110,000 g/mol linear hPS sample is more comparable with that of the linear dPS (MW = 114,000 g/mol) characterized here, making it a useful benchmark for comparison. Using their parameterization of the 110,000 g/mol linear hPS sample, we calculate that its %FV is equal to 12.2%, which is reasonably close to the 11.9% FV of our 460,000 g/mol linear hPS sample. Therefore, we do not observe a notable difference in our pure component characterizations of PS samples when the MWs are greater than 100,000 g/mol and compared over the same T and P ranges [note: MW does affect LCL model characterizations as the sample MW approaches the oligomeric regime, where chain ends play an increasingly important role in influencing microscopic behavior].

When PS is branched, however, deuterium labeling has a weaker effect on %FV, which increases by about 0.5% from star hPS to star dPS. These results suggest that for star PS, deuterium labeling enhances the degree of intermolecular penetration into the densely populated region of segments near the star core, thus facilitating more efficient molecular packing and reducing the %FV of star dPS in comparison to linear dPS. To our knowledge, we are reporting for the first time that the effect of deuterium labeling on the pure component properties (e.g. % free volume, thermal expansion coefficient) is diminished in the case of star dPS, relative to its linear analog. Note that our conclusions are drawn directly from analyses of experimental data for the pure states, whereas other studies in the literature have focused on measurements of the mixed state.

Having compared the pure component properties of the linear and star PS samples with PVME, in the next section, we analyze the pure linear and star isotopic PS samples.

3.3. Comparisons of Pure Isotopic Linear and Star PS Samples

Once again, our route to understanding mixtures begins with an analysis of pure component properties. Here we compare pairs of linear and star isotopic PS samples, which consist of both an unlabeled and a deuterium labeled PS component; e.g., linear hPS/linear dPS. These mixtures are distinct from the LCST-type PS/PVME blends described in the previous section, because isotopic PS mixtures undergo UCST-type phase separation. Correspondingly, we find that a different pure component property analysis provides insight about UCST-type isotopic PS mixture compatibility. Below we will comment on the relative compatibility of the isotopic PS pairs using the LCL theory, however, it is useful to begin by summarizing the experimental and simulation results.

SANS measurements performed by Bates and Wignall [25] on a linear hPS/linear dPS blend, where the MWs of both species were ~1,000,000 g/mol, indicated UCST-type phase separation at a temperature of ~433 K. Further investigation of isotopic PS blends by Greenberg and coworkers [5] included SANS measurements of blends containing 4-arm star hPS and dPS. In their work, comparisons of the Flory-Huggins χ-parameters as a function of temperature suggested the following order of compatibility (from least to most

compatible): star dPS/linear hPS, star hPS/linear dPS, linear hPS/linear dPS [there were no measurements reported for a star hPS/star dPS blend] [5]. Furthermore, they reported that χ decreases with increasing T for all of the isotopic blends. These results suggest UCST-type behavior, which support the observations of Bates and Wignall described above, although no phase separation of the star mixtures was observed due to the low MWs (~100,000 g/mol) of the polymers.

In a simulation study by Theodorakis and coworkers, [16] the relative compatibility of mixtures of linear and star branched chains were probed via a Monte Carlo/bond fluctuation model (BFM) based approach. They considered a general category of chain mixtures in which the interaction energies between beads on chains of the same 'type' were neutral (i.e., $\varepsilon_{AA} = \varepsilon_{BB} = 0$) and where heterocontacts were repulsive (i.e., $\varepsilon_{AB} > 0$) [16]. Although their results are not intended to map to a specific experimental system, and do not account for the effects of deuterium labeling, the relative compatibilities of the simulated linear/linear, linear/branched, and branched/branched mixtures show the same ordering as the experimental results for isotopic PS blends reported by Greenberg and coworkers [5].

We have found that a comparison of the pure component %FVs for UCST-type blends does not serve as a useful predictor of miscibility. This is because differences in pure component %FVs are associated with an unfavorable contribution to the excess *entropy* of mixing, thus they track well with trends in LCST behavior. UCST-type blends, however, have an unfavorable *enthalpic* contribution to the free energy of mixing. White and Lipson [32,63] have proposed that a comparison of the cohesive energy densities (CEDs) serves as a better guide for predicting pure component compatibility in these cases [we refer the reader to section 2.3 for more detail]. We also point out that LCL model calculations indicate that %FV is not correlated with CED; thus the CED serves as a separate metric for making predictions about pure component compatibility. In Figure 3, we rank the CEDs of the PS samples to illustrate the best 'matches' between isotopic pairs.

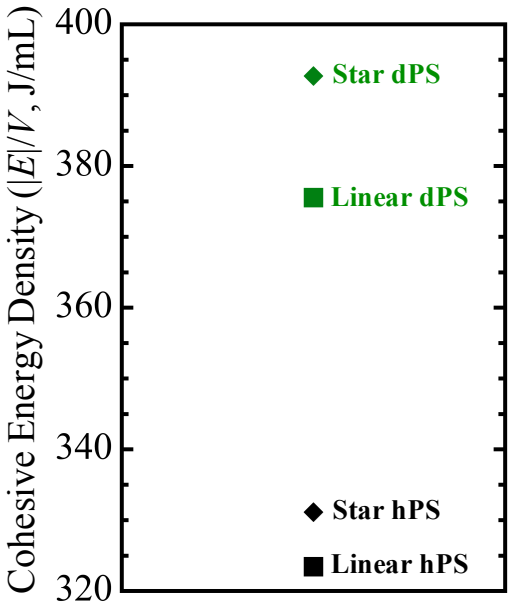

Figure 3. Ranking of the linear PS and star PS CEDs calculated for T = 400 K and P = 1 atm.

Figure 3 indicates that branching has a weak effect on CED (8 J/mL increase) when comparing between linear hPS and star hPS, while deuterium labeling yields a notable change in CED, which increases by 53 J/mL from linear hPS to linear dPS. The value of the CED is primarily influenced by two factors: the number of theoretical segments per mass (r/MW) and the strength of the non-bonded segmental interactions ($|\varepsilon|$) (see Section 2.3), such that the product of r/MW and $|\varepsilon|$ is proportional to the CED. Deuterium labeling increases the CED of PS because the number of theoretical segments per mass increases from linear hPS to dPS, which overcomes the reduction in the strength of the non-bonded segmental interactions caused by deuterium labeling.

When combined with branching, the results shown in Figure 3 suggest that deuterium labeling and branching have an additive effect on the CED, which increases by 23 J/mL from linear to star dPS. In this case, there is small increase in the number of theoretical segments per mass from linear to star dPS, in addition to a ~50 J/mol increase in the non-bonded interaction energy (see Table 1). Therefore, our analysis indicates that the combined effect of branching and deuterium labeling has a stronger effect on CED than deuterium labeling, alone. In fact, this conclusion is consistent with χ based analyses of branched and deuterium labeled systems of PB [27] and PS [5], which reported that the

combined effects of branching and deuterium labeling induced a stronger shift in χ than the isolated effect of deuterium labeling.

There are four possible pure component pairs in which one component is deuterated, and therefore accessible to SANS experiments. The pure component pairs in order of decreasing CED difference, which should track from least to most compatible, are as follows: star dPS and linear hPS (70 J/mL), star hPS and star dPS (62 J/mL), linear hPS and linear dPS (53 J/mL), star hPS and linear dPS (45 J/mL). If we identify the least compatible pair as the one for which we find the greatest CED difference then that would be star dPS and linear hPS (70 J/mL) and, indeed, the experimental SANS data yielded the most unfavorable χ-parameter values for the star dPS/linear hPS blend. Next would come star hPS and star dPS (62 J/mL), however, there are no experimental measurements for the star hPS/star dPS blend. Finally, we would predict the star hPS/linear dPS blend (45 J/mL) to be the most compatible of the isotopic blends, having a CED difference slightly smaller than that for linear hPS/linear dPS (53 J/mL). In fact, experimental observations would reverse this last ranking on the basis of the experimentally derived estimates for χ. While not a perfect match with χ estimates, our miscibility predictions based on pure component CEDs suggests a qualitative trend that agrees fairly well with the experimental observations of Greenberg and coworkers [5].

4. Blend Modeling

4.1. Blend Miscibility

Here we distinguish between predicting blend miscibility trends using pure component analysis, and modeling the blend, itself. When modeling a blend, we use a v value that is the arithmetic average of the pure component v values; the r parameter is then adjusted such that the pure component hard core volumes, rv, are unchanged for the molecular weight associated with the experimental PVT data that were analyzed. In addition, as described at the start of Section 2.2, if the molecular weight of a blend constituent differs from that of the pure component analysis, then the r parameter is

appropriately scaled without any changes in v. The final parameter to be fixed when modeling the blend is g, which characterizes the strength of the mixed interactions, ε_{ij}, by scaling the geometric mean of the pure component ε values ($\varepsilon_{ij} = g(\varepsilon_{ii}\varepsilon_{jj})^{1/2}$) so as to match some experimental data associated with blend behavior. In this work we fixed g in each case for which experimental LCST data were available so that the value calculated using the LCL theory matched the experimental result.

The parameters used to model the linear and star PS blends with PVME are tabulated in Table 2, which is divided into two major sections: the upper section of Table 2 lists the parameters for modeling the linear and star *hPS* blends with PVME, and the lower section of Table 2 gives the parameters for modeling the linear and star *dPS* blends with PVME. Each major section is further divided by the MW of the PS blend component: high MW PS (MW ≈ 275,000 g/mol) and low MW PS (MW ≈ 120,000 g/mol).

Also, note that all of the g parameter values listed in Table 2 are greater than unity, which means that the mixed interaction strength needed to capture the experimental phase separation behavior is stronger than would be found using the geometric mean approximation; this is characteristic of all LCST blends we have studied [59].

Blend	MW of PS (g/mol)	r (PS)/r (PVME)	v (mL/mol)	$\lvert \varepsilon_{PS} - \varepsilon_{PVME} \rvert$ (J/mol)	Experimental LCST (K)	g
Linear hPS/PVME	275,000	25177.6/9279.5	9.4984	175.8	386[a]	1.00097
Star hPS/PVME	255,000	23663.7/9445.5	9.3314	169.4	383[a]	1.00089
Linear hPS/PVME	120,000	10986.6/9279.5	9.4984	175.8	394[b]	1.00096
Star hPS/PVME	120,000	11135.8/9445.5	9.3314	169.4	---	---
Linear dPS/PVME	255,000	24051.2/10469.7	8.4186	68.1	427[c]	1.000123
Star dPS/PVME	255,000	24091.5/10515.2	8.3822	118.3	---	---
Linear dPS/PVME	119,000	11223.9/10469.7	8.4186	68.1	439[b]	1.000099
Star dPS/PVME	119,000	11242.7/10515.2	8.3822	118.3	---	---

Table 2. Molecular weights and corresponding molecular parameters for modeling the PS/PVME blends. For each blend, the experimental LCST and *g* parameter value fit to the experimental LCST is also listed. The experimental LCSTs can be found in refs. [12], [74], and [35] for superscripts a, b, and c, respectively

As summarized in the *hPS/PVME* (upper) section of Table 2, blends of linear hPS and star hPS with PVME exhibit essentially the same LCST values (386 K and 383 K, respectively) [12] and thus require *g* values that are roughly equivalent to model the blends (g = 1.00097 and 1.00089, respectively). This behavior is consistent with the results shown in Figure 1, where the temperature dependence of the experimentally determined specific volumes of the two polymers are extremely close; correspondingly, so are the LCL predictions for their pure component properties, e.g. their %FV values calculated at 400 K and 1 atm. Therefore, linear and star hPS behave similarly in their pure states and upon mixing with PVME.

Now consider the effect of decreasing the MW of the PS component. The experimentally measured LCST [74] listed for the lower MW linear hPS/PVME blend is 394 K, ~8 K greater than the higher MW blend (386 K); i.e., reducing the MW of linear hPS from 275,000 g/mol to 120,000 g/mol slightly enhances its miscibility with PVME. This behavior can be attributed to a favorable increase in the ideal (or combinatorial) entropic contribution to the free energy of mixing upon lowering the MW, which is reflected in the smaller *r* parameter value listed in Table 2 for the lower MW linear hPS blend constituent, relative to the corresponding value for the higher MW linear hPS blend. Also note that approximately the same *g* value (g = 1.00096) can be used to model both the high and low MW linear hPS blends [in fact, using the *g* value for the higher MW linear hPS blend (g = 1.00097) would predict an LCST = 398 K for the lower MW linear hPS blend]. There is no experimentally measured LCST for the remaining blend in this section, i.e. the lower MW star hPS/PVME blend. We will return to this blend shortly and provide a prediction for its LCST.

Next we to turn to the results listed in the *dPS/PVME* (lower) section of Table 2, which illustrate the effect of going from linear hPS to linear dPS on the LCST value of the blend with PVME. Experimental cloud point data indicate that deuterium labeling raises

the LCST by ~40 K from that of the corresponding linear hPS/PVME blend [35,36]. Also note that the low MW linear dPS/PVME blend is ~12 K more miscible than the high MW linear dPS/PVME blend, which again can be rationalized by the favorable increase in the ideal (or combinatorial) entropic contribution to the free energy of mixing by lowering the MW of dPS. The experimentally observed change in blend miscibility upon deuterium labeling is consistent with the results shown in Figure 1 and described section 3.1; i.e., there is a notable shift in the *PVT* behavior of linear dPS relative to linear hPS. As a result, the LCL model predictions for the pure component properties of linear dPS, such as %FV and the thermal expansion coefficient, are larger than those of linear hPS at 400 K and 1 atm, and closer in value to those of PVME.

The results tabulated in Table 2 indicate that the change in the pure component properties upon deuterium labeling also manifests in the blends, where we find that a smaller g value (g = 1.000123) captures the experimental LCST of linear dPS/PVME than the g value needed to model the linear hPS/PVME blend (g = 1.00097). White and Lipson [59] have illustrated in previous work that g values are linearly correlated with $| \varepsilon_{ii} - \varepsilon_{jj} |$ for LCST-type blends. Consistent with their observation, we find in this work that the unique g values needed to model linear hPS/PVME versus linear dPS/PVME are connected to the distinct $| \varepsilon_{ii} - \varepsilon_{jj} |$ values for these blends, which are 175.8 J/mol and 68.1 J/mol, respectively. The implications of the different $| \varepsilon_{ii} - \varepsilon_{jj} |$ and g values on the relative thermodynamics of mixing for these blends are described in detail in section 4.2.

The remaining blends listed in the lower section of Table 2 are star dPS/PVME blends, and our goal in the following paragraphs is to summarize the available experimental information about the combined effects of deuterium labeling and branching on blend miscibility from the literature. We begin by highlighting the limited experimental evidence that suggests the miscibility of star dPS/PVME is enhanced relative to that of linear hPS/PVME. In a study by Gomez-Elvira and coworkers, [26] they concluded from cloud point measurements that the LCST of a *partially* deuterium labeled 6-arm star PS sample (MW = 1,500,000 g/mol) blended with PVME was ~6 K greater than that of an analogous linear hPS/PVME blend. In their case, only a partially deuterium labeled star molecule

was available, which consisted of a 6-arm star PS sample for which a 'block' region at the chain end of each star arm was deuterium labeled [26]. The deuterium labeled blocks comprised ~16% of the total mass of the star polymer [26].

To our knowledge, work published by Russell et al. [36] is the only example in the literature for which the miscibility of a fully deuterium labeled 4-arm star PS/PVME blend was measured. First, to isolate the effect of branching, they performed cloud point measurements on an unlabeled 4-arm star hPS(MW = 221,000 g/mol)/PVME(MW = 149,000 g/mol) blend and found that its LCST was ~10 K greater than that of an analogous linear hPS/PVME blend [36]. In contrast, the measurements reported by Pavawongsak et al.[12] for a comparable 4-arm star hPS/PVME blend indicated that its LCST was essentially the same as that of an analogous linear hPS/PVME blend. It is possible that the heating rates used by Russell and coworkers (1 – 10 K/min), which were an order of magnitude faster than those used by Pavawongsak et al. (0.01 – 0.5 K/min), may have contributed to this difference. In fact, there is some evidence in the literature that suggests that faster heating rates tend to yield higher cloud point temperatures measurements [75]. However, the set of measurements performed by Russell and coworkers is *internally* consistent, and thus still insightful. Their investigation of the combined effects of branching and deuterium labeling indicated that the LCST for 4-arm star dPS (MW = 211,000 g/mol)/PVME (MW = 149,000 g/mol) was ~20 K greater than that of an analogous linear hPS/PVME blend [36]. Therefore, their results suggest that the combination of branching and deuterium labeling may produce a noticeable shift in miscibility.

Graessley and coworkers [27] also considered the combined effect of branching and deuterium labeling; they studied a series of polybutadiene (PB) homopolymer blends where the extent of branching and the component that was deuterium labeled were systematically varied. Using SANS measurements of these blends, they observed consistent behavior in the Flory-Huggins χ-parameter value, i.e. shifts that depended on whether the more, or less, branched component was deuterium labeled. They found χ increased (reduced miscibility) when the more branched component was deuterium labeled and decreased (enhanced miscibility) when the less branched component was deuterium

labeled. Furthermore, they found that the arithmetic average of the χ values of these blends was approximately equal to the χ value of the blend in which both components were unlabeled; i.e. the χ values of the differently labeled blends "bracketed" the χ value of the unlabeled blend.

As discussed in Section 3.2, the pure component properties of star dPS are 'bracketed' by those of linear dPS and star hPS. Using the LCL theory, we can determine if this bracketing behavior extends to the star dPS/PVME blend, and see the consequences on the thermodynamics of mixing.

4.2. Thermodynamics of Mixing

We now turn from miscibility predictions to the underlying thermodynamics of the PS/PVME mixtures, such as the enthalpic and entropic contributions to the free energies of mixing. In previous work, White and Lipson [61] demonstrated that for LCST mixtures the magnitude of the enthalpic contribution to the free energy of mixing is controlled by the g parameter. On the other hand, the difference in the pure component component ε values, $| \varepsilon_{ii} - \varepsilon_{jj} |$, controls the excess (non-combinatorial) entropic contribution, which for high MW blends accounts for almost all of the total entropy change upon mixing [61]. We have used our LCL theory to gain further insight about the underlying thermodynamic behavior of mixtures by calculating ΔH_{mix} and $T\Delta S_{mix}$ for a number of polymer solutions and blends [32,58,61,62].

In this work, we have applied the same approach for the linear and star PS/PVME blends of interest here. Figure 4 illustrates our predictions for the combined effect of branching and deuterium labeling on ΔH_{mix} and $T\Delta S_{mix}$ for the high MW PS/PVME blends. Note that our calculations for the star dPS/PVME blend use values of g that were fit to the experimental LCSTs of the *other* PS/PVME blends. In the absence of an experimental measurement of the star dPS/PVME blend LCST, we provide predictions for the star dPS/PVME blend in Figure 4 by assuming that its miscibility is in the range of the other PS/PVME blends. This assumption is supported by our pure component based analysis

described in Section 3.2, as well as the experimental evidence from the literature [27,36] that was summarized in the previous section.

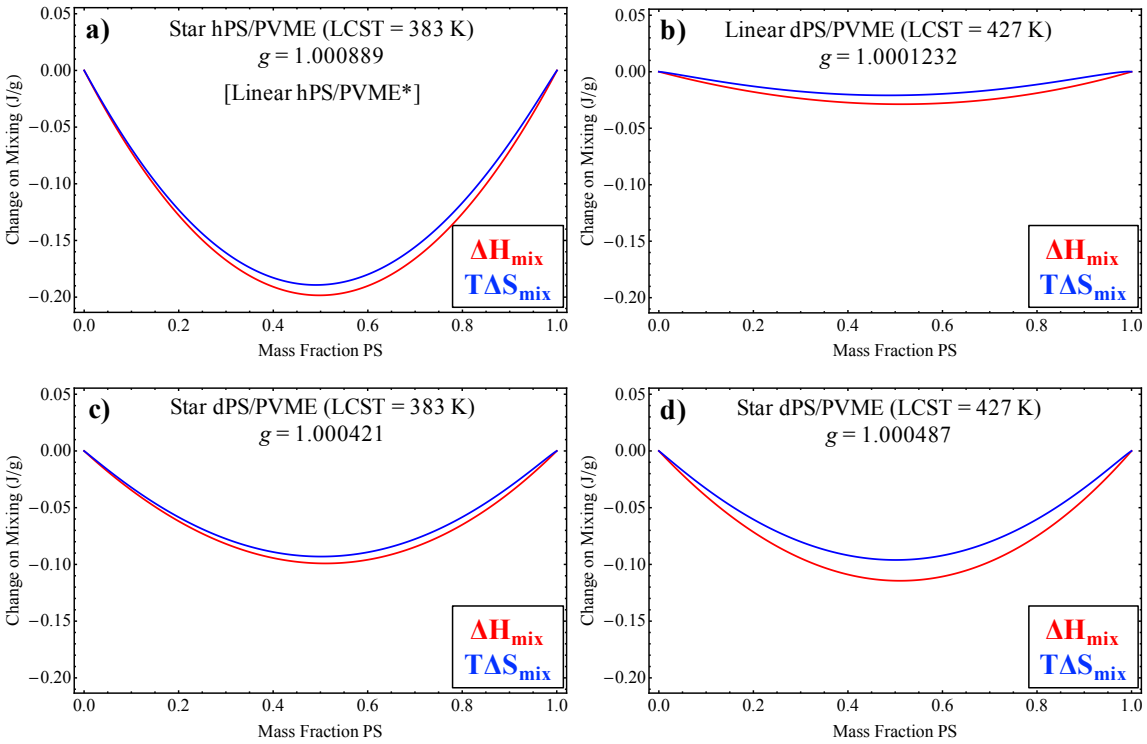

Figure 4. Enthalpic and entropic contributions to the free energies of mixing for PS (MW = 255,000 g/mol) blends with PVME, calculated for 380 K and 1 atm. In both a) and b), *g* values correspond to those that yield the experimental blend LCSTs for star hPS/PVME and linear dPS/PVME, respectively. In c) and d), the *g* values correspond to those that yield LCSTs for star dPS/PVME which, match those of star hPS/PVME and linear dPS/PVME, respectively. Curves: ΔH_{mix} – red and $T\Delta S_{mix}$ – blue. [* - the values of ΔH_{mix} and $T\Delta S_{mix}$ for linear hPS/PVME are approximately the same as those for star hPS/PVME, thus the calculations for linear hPS/PVME are not shown in a) for the purpose of clarity].

First, we consider the effect of deuterium labeling on the values of ΔH_{mix} and $T\Delta S_{mix}$ for PS/PVME by comparing the LCL model predictions for the star hPS/PVME (Figure 4a) and linear dPS/PVME (Figure 4b) blends. We have chosen to use the star hPS/PVME blend calculations for this analysis, because the values of ΔH_{mix} and $T\Delta S_{mix}$ for the star hPS/PVME blend are essentially equal to those of the linear hPS/PVME blend [the results for the linear hPS/PVME blend are omitted from Figure 4 for the sake of clarity]. This

behavior is consistent with the g and $|\ \varepsilon_{ii} - \varepsilon_{jj}\ |$ values for the linear and star hPS/PVME blends, which are approximately equal for these blends (see Table 2). Another reason for providing the LCL model calculations for the star hPS/PVME blend in Figure 4 is that they will be used to make comparisons with our predictions for the star dPS/PVME blend, which will be addressed shortly.

A comparison of the results shown in Figures 4a and 4b indicates that the entropic penalty of mixing is less *un*favorable for linear dPS/PVME than star hPS/PVME, and the enthalpy of mixing is less favorable for linear dPS/PVME than star hPS/PVME. As described above, the value of $|\ \varepsilon_{ii} - \varepsilon_{jj}\ |$ is proportional to the magnitude of the unfavorable entropic contribution to the free energy of mixing for LCST-type mixtures [61,62]. Recall that in Section 3.2, we concluded that deuterium labeling reduced the value of $|\ \varepsilon\ |$ and increased the %FV of linear dPS in comparison to the unlabeled linear and star hPS samples. In other words, deuterium labeling shifts the pure component properties closer to those of PVME, making the linear dPS sample a better match with PVME than the unlabeled linear and star molecules. In ref. [61], White et al. explored the effect of a hypothetical 25% reduction in the value of $|\ \varepsilon_{ii} - \varepsilon_{jj}\ |$ on $T\Delta S_{mix}$ for hPS/PVME, and found that it yielded a ~30% reduction in the entropic penalty of mixing. In this work, we find a ~60% shift in the value of $|\ \varepsilon_{ii} - \varepsilon_{jj}\ |$ upon deuterium labeling, which suggests that the entropic penalty of mixing is notably reduced for linear dPS/PVME in comparison to star hPS/PVME. Finally, the value of g, which controls the magnitude of ΔH_{mix}, was fit to the experimental LCST for each blend. The value of g which yields the experimental LCST for linear dPS/PVME is smaller than the g value that yields the experimental LCST for star hPS/PVME, thus the mixed interactions are weaker in the linear dPS/PVME blend and its enthalpy of mixing is less favorable than that of star hPS/PVME.

Turning to Figures 4c and 4d, two sets of predictions for the values of ΔH_{mix} and $T\Delta S_{mix}$ for the star dPS/PVME blend are illustrated. In Figure 4c, we model the star dPS/PVME blend such that its LCST matches that of the star hPS/PVME blend (383 K), while in Figure 4d, we model the star dPS/PVME blend such that its LCST matches that of the linear dPS/PVME blend (427 K). These two scenarios represent predictions for the

star dPS/PVME blend under the condition that its miscibility is equivalent to either the least miscible (star hPS/PVME) or most miscible (linear dPS/PVME) blend of the set of PS/PVME blends.

Note that between Figures 4c and 4d, $T\Delta S_{mix}$ does not change because it is controlled by the value of $| \varepsilon_{ii} - \varepsilon_{jj} |$, which is determined by fitting the LCL EOS to the pure component *PVT* data. Our predictions for the star dPS/PVME blend indicate that $T\Delta S_{mix}$ is less *un*favorable than that of star hPS/PVME (Figure 4a) and more unfavorable than that for linear dPS/PVME; i.e., $T\Delta S_{mix}$ for star dPS/PVME is 'bracketed' by the values of $T\Delta S_{mix}$ for the star hPS/PVME and linear dPS/PVME blends. This is consistent with our calculations of the pure component properties of star dPS relative to star hPS and linear dPS (see Section 3.2). For example, Figure 2 showed that our calculated %FV for star dPS was 0.5% *more* than that of star hPS and 0.5% *less* than that of linear dPS. The relative $T\Delta S_{mix}$ for the star dPS/PVME blend in comparison to the star hPS/PVME and linear dPS/PVME blends can be rationalized in terms of the pure component %FVs (or equivalently, thermal expansion coefficients): the combination of branching and deuterium labeling reduces the %FV of star dPS relative to linear dPS, which is a shift in %FV away from that of PVME (and toward that of star hPS). Thus star dPS is more of a mismatch with PVME in terms of %FV than linear dPS, but a better match than star hPS, which results in the 'bracketing' of its $T\Delta S_{mix}$.

The only change that occurs between Figures 4c and 4d is our prediction of ΔH_{mix} for star dPS/PVME. Recall that the magnitude of ΔH_{mix} is controlled by the value of g, which was adjusted in each case to yield an LCST for the star dPS/PVME blend that matched that of the star hPS/PVME blend (Figure 4c) and linear dPS/PVME (Figure 4d) blend. Both sets of predictions for the star dPS/PVME blend indicate that ΔH_{mix} for the star dPS/PVME blend is *less* favorable than star hPS/PVME (Figure 4a) and *more* favorable than linear dPS/PVME (Figure 4b). We tested the robustness of our predictions for ΔH_{mix} of the star dPS/PVME blend by determining the values of g that yield enthalpy changes upon mixing that match those of the star hPS/PVME and linear dPS/PVME blends.

The ΔH_{mix} of star dPS/PVME matches that of star hPS/PVME (linear dPS/PVME) for $g \approx 1.00080$ ($g \approx 1.00003$), which predicts an LCST = 580 K (181 K) using the LCL theory. Under these criteria, the LCL theory predicts that the LCST of star dPS/PVME must lie ~200 K away from the LCSTs of the other PS/PVME blends. This is unlikely given our pure component property based analysis for the set of the PS samples, which tracks well with the experimental miscibility trends. Therefore, we predict that ΔH_{mix} for star dPS/PVME is 'bracketed' by the values of ΔH_{mix} for the star hPS/PVME and linear dPS/PVME blends.

In summary, we find that the differences in the pure component properties of star dPS relative to those of star hPS and linear dPS, yield a notable difference in the thermodynamics of mixing with PVME. Our results suggest that branching reduces the effect of deuterium labeling on ΔH_{mix} and $T\Delta S_{mix}$ when compared with a chemically identical linear molecule analog, such that ΔH_{mix} and $T\Delta S_{mix}$ for star dPS/PVME are bracketed by the corresponding values for the star hPS/PVME and linear dPS/PVME blends.

5. Conclusions

We have used the Locally Correlated Lattice (LCL) theory to study the individual and combined effects of branching and deuteration on the properties and miscibility of polystyrene (PS). We believe that this is the first time that a theoretical study has calculated such properties directly from experimental data for the pure states. Our finding is that the combination of 4-arm star branching and deuterium labeling yields a detectable change in the properties of pure PS, which affects its compatibility with PVME (an LCST-type mixture) and isotopic variants of PS (an UCST-type mixture). We used two independent metrics to predict LCST-type vs. UCST-type mixture compatibility: percent free volumes (%FVs) and cohesive energy densities (CEDs), respectively. Using these approaches, our predicted miscibility trends tracked well with experimental measurements available in the literature.

We have recently been energetic in testing the extent to which the LCL theory could be used in correlating pure component properties, alone, to predict miscibility. Thus, one route we used here began with fitting our LCL equation of state (EOS) to experimental *PVT* data for PS samples that were branched, deuterated, or both, as well as linear samples. These data reflected some interesting differences between samples, for example a shift in $V(T)$ at atmospheric pressure between linear and 4-arm star dPS that was not present between linear and 4-arm star hPS. This behavior was reflected in our calculations for the pure component cohesive energy densities (CED) and our predictions for the percent free volumes (%FV). We found differences in each property between linear and star dPS, while the values for linear and star hPS were essentially equal.

Our recent work on different polymeric systems leads us conclude that CED and %FV can be useful tools, but under different circumstances. For example, %FV is a useful metric for LCST-type mixtures because of its connection with the unfavorable entropic contribution to the free energy of mixing [60-62]. In addition to %FV, other pure component properties such as the non-bonded nearest neighbor interaction energy ($|\varepsilon|$) and the thermal expansion coefficient (α), which are correlated with %FV, also influence LCST-type miscibility. We predict that the %FV, $|\varepsilon|$, and α of star dPS are more of a mismatch with those of PVME relative to those of a linear dPS sample with comparable molecular weight, which indicates that star dPS is less compatible with PVME than linear dPS.

We next turned to the isotopic mixture of hPS and dPS. For UCST-type mixtures such as these CED values are a better a guide for predicting compatibility because of their connection with the unfavorable enthalpic contribution to the free energy of mixing [60]. We calculated that the CED of star dPS is more of a mismatch with that of linear hPS than with linear dPS, which suggests that star dPS is less compatible with its linear hydrogenated counterpart than with the analogous h-star. This shift in CED upon deuterium labeling and branching is driven by changes in the number of segments per mass and the non-bonded interaction energy, the product of which tracks with CED. The trend in mixture

compatibility that we have reported in this work is in good agreement with available experimental/simulation information from the literature [5].

A more common route to understanding the underlying origins of miscibility is to model the mixtures, themselves. We applied our LCL theory to a series of PS/PVME blends in order to gain insight about how the key contributions to the thermodynamics of mixing are influenced by the combination of 4-arm star branching and deuterium labeling. For the star dPS/PVME blend, we calculated its enthalpy and entropy change upon mixing based on the prediction from our pure component analysis that its miscibility is in the range of the other PS/PVME blends. One conclusion is that the enthalpy of mixing is more favorable, but the entropic penalty leads to the entropy of mixing to be more unfavorable for star dPS/PVME than for linear dPS/PVME. Further, the values of these thermodynamic quantities for the star dPS/PVME blend lie roughly between those for the linear dPS/PVME and star hPS/PVME blends. These bounds are consistent with our pure component property based analysis, where we found that the non-bonded interaction energy and %FV values for star dPS are approximately the arithmetic average of the values for linear dPS and star hPS. Thus, the shifts in the thermodynamics of mixing for star dPS/PVME relative to the other PS/PVME blends are driven by the differences in the pure component properties of star dPS in comparison to the other PS samples.

Acknowledgements

We acknowledge financial support from NSF DMR-1403757 to J.E.G.L. and Graduate Assistance in Areas of National Need (GAANN) to J.D.

References

[1] Browarzik, D.; Langenbach, K.; Enders, S.; Browarzik, C. Modeling of the branching influence on liquid-liquid equilibrium of binary and ternary polymer solutions by lattice-cluster theory. *Journal of Chemical Thermodynamics* **2013***, 62*, 56-63.

[2] Eckelt, J.; Samadi, F.; Wurm, F.; Frey, H.; Wolf, B. A. Branched Versus Linear Polyisoprene: Flory-Huggins Interaction Parameters for their Solutions in Cyclohexane. *Macromolecular Chemistry and Physics* **2009***, 210*, 1433-1439.

[3] Fan, W.; Zheng, S. Miscibility and crystallization behavior in blends of poly(methyl methacrylate) and poly(vinylidene fluoride): Effect of star-like topology of poly(methyl methacrylate) chain. *Journal of Polymer Science Part B-Polymer Physics* **2007***, 45*, 2580-2593.
[4] Fredrickson, G. H.; Liu, A. J.; Bates, F. S. Entropic Corrections to the Flory-Huggins Theory of Polymer Blends - Architectural and Conformational Effects. *Macromolecules* **1994***, 27*, 2503-2511.
[5] Greenberg, C. C.; Foster, M. D.; Turner, C. M.; Corona-Galvan, S.; Cloutet, E.; Butler, P. D.; Hammouda, B.; Quirk, R. P. Effective interaction parameter between topologically distinct polymers. *Polymer* **1999***, 40*, 4713-4716.
[6] Greenberg, C. C.; Foster, M. D.; Turner, C. M.; Corona-Galvan, S.; Cloutet, E.; Quirk, R. P.; Butler, P. D.; Hawker, C. Effective interaction parameter between branched and linear polystyrene. *Journal of Polymer Science Part B-Polymer Physics* **2001***, 39*, 2549-2561.
[7] Huang, C. F.; Kuo, S. W.; Lin, H. C.; Chen, J. K.; Chen, Y. K.; Xu, H. Y.; Chang, F. C. Thermal properties, miscibility and specific interactions in comparison of linear and star poly(methyl methacrylate) blend with phenolic. *Polymer* **2004***, 45*, 5913-5921.
[8] Lee, J. S.; Foster, M. D.; Wu, D. T. Effects of branch points and chain ends on the thermodynamic interaction parameter in binary blends of regularly branched and linear polymers. *Macromolecules* **2006***, 39*, 5113-5121.
[9] Martter, T. D.; Foster, M. D.; Yoo, T.; Xu, S.; Lizarraga, G.; Quirk, R. P. Thermodynamic interaction parameter of star-star polybutadiene blends. *Journal of Polymer Science Part B-Polymer Physics* **2003***, 41*, 247-257.
[10] Martter, T. D.; Foster, M. D.; Yoo, T.; Xu, S.; Lizzaraga, G.; Quirk, R. P.; Butler, P. D. Nonuniversal behavior of the thermodynamic interaction parameter in blends of star and linear polybutadiene. *Macromolecules* **2002***, 35*, 9763-9772.
[11] Okumoto, M.; Iwamoto, Y.; Nakamura, Y.; Norisuye, T. Excluded-volume effects in star polymer solutions. Six-arm star polystyrene in benzene. *Polym. J.* **2000***, 32*, 422-427.
[12] Pavawongsak, S.; Higgins, J. S.; Clarke, N.; McLeish, T. C. B.; Peiffer, D. G. Phase separation in entangled polystyrene/poly(vinyl methyl ether) blends. *Polymer* **2000***, 41*, 757-763.

[13] Santore, M. M.; Han, C. C.; Mckenna, G. B. A Comparison of the Thermodynamic Stability and Phase-Separation Kinetics of Polymer Blends Containing Cyclic Chains of High-Molecular-Weight. *Macromolecules* **1992**, *25*, 3416-3423.
[14] Shen, J.; Zheng, S. X. Comparative studies on miscibility and phase behavior of linear and star poly(2-methyl-2-oxazoline) blends with poly(vinylidene fluoride). *Journal of Polymer Science Part B-Polymer Physics* **2006**, *44*, 942-952.
[15] Sremcich, P. S.; Faust, A. B.; Gilmer, J. W.; Mays, J. W. Influence of Star Polymer Functionality on the Core Exclusion Exhibited in Melt Blends. *Polymer Communications* **1989**, *30*, 146-149.
[16] Theodorakis, P. E.; Avgeropoulos, A.; Freire, J. J.; Kosmas, M.; Vlahos, C. Monte Carlo simulation of star/linear and star/star blends with chemically identical monomers. *Journal of Physics-Condensed Matter* **2007**, *19*, 466111.
[17] Wolf, B. A. Polymer-polymer interaction: Consistent modeling in terms of chain connectivity and conformational response. *Macromolecular Chemistry and Physics* **2006**, *207*, 65-74.
[18] Wu, Y.; Newkirk, M. S.; Dudek, S. T.; Williams, K.; Krukonis, V.; McHugh, M. A. Architectural Effects on the Solution Behavior of Linear and Star Polymers in Propane at High Pressures. *Ind Eng Chem Res* **2014**, *53*, 10133-10143.
[19] Xiong, X.; Eckelt, J.; Wolf, B. A. Linear versus Three-Arm Star Polybutadiene: Effects of Polymer Architecture on the Thermodynamic Solution Behavior. *Macromolecules* **2012**, *45*, 9539-9546.
[20] Zhao, J.; Sakellariou, G.; Green, P. F. Phase behavior of diblock copolymer/star-shaped polymer thin film mixtures. *Soft Matter* **2016**, *12*, 3849-3853.
[21] Zhao, L.; Li, Y.; Zhong, C. Integral equation theory study on the phase separation in star polymer nanocomposite melts. *J. Chem. Phys.* **2007**, *127*, 154909.
[22] Arya, G.; Panagiotopoulos, A. Impact of branching on the phase behavior of polymers. *Macromolecules* **2005**, *38*, 10596-10604.
[23] Yang, J.; Peng, C.; Liu, H.; Hu, Y.; Jiang, J. A generic molecular thermodynamic model for linear and branched polymer solutions in a lattice. *Fluid Phase Equilib.* **2006**, *244*, 188-192.

[24] Theodorakis, P.; Avgeropoulos, A.; Freire, J.; Kosmas, M.; Vlahos, C. Effects of the chain architecture on the miscibility of symmetric linear/linear and star/star polymer blends. *Macromolecules* **2006***, 39*, 4235-4239.
[25] Bates, F. S.; Wignall, G. D. Nonideal Mixing in Binary Blends of Perdeuterated and Protonated Polystyrenes. *Macromolecules* **1986***, 19*, 932-934.
[26] Gomez-Elvira, J. M.; Halary, J. L.; Monnerie, L.; Fetters, L. J. Isotope Effects on the Phase-Separation in Polystyrene Poly(vinyl Methyl-Ether) Blends .2. Influence of the Microstructure of Linear and Star Block-Copolymers. *Macromolecules* **1994***, 27*, 3370-3375.
[27] Graessley, W. W.; Krishnamoorti, R.; Balsara, N. P.; Fetters, L. J.; Lohse, D. J.; Schulz, D. N.; Sissano, J. A. Effect of Deuterium Substitution on Thermodynamic Interactions in Polymer Blends. *Macromolecules* **1993***, 26*, 1137-1143.
[28] Nedoma, A. J.; Lai, P.; Jackson, A.; Robertson, M. L.; Wanakule, N. S.; Balsara, N. P. Phase Diagrams of Blends of Polyisobutylene and Deuterated Polybutadiene as a Function of Chain Length. *Macromolecules* **2011***, 44*, 3077-3084.
[29] Rhee, J.; Crist, B. Isotope and Microstructure Interactions in Blends of Random Copolymers. *J. Chem. Phys.* **1993***, 98*, 4174-4182.
[30] Sakai, V. G.; Maranas, J. K.; Peral, I.; Copley, J. R. D. Dynamics of PEO in blends with PMMA: Study of the effects of blend composition via quasi-elastic neutron scattering. *Macromolecules* **2008***, 41*, 3701-3710.
[31] Schwahn, D.; Hahn, K.; Streib, J.; Springer, T. Critical Fluctuations and Relaxation Phenomena in the Isotopic Blend Polystyrene Deuteropolystyrene Investigated by Small-Angle Neutron-Scattering. *J. Chem. Phys.* **1990***, 93*, 8383-8391.
[32] White, R. P.; Lipson, J. E. G.; Higgins, J. S. Effect of Deuterium Substitution on the Physical Properties of Polymer Melts and Blends. *Macromolecules* **2010***, 43*, 4287-4293.
[33] Yurekli, K.; Krishnamoorti, R. Thermodynamic interactions in blends of poly(4-tert-butyl styrene) and polyisoprene by small-angle neutron scattering. *Journal of Polymer Science Part B-Polymer Physics* **2004***, 42*, 3204-3217.
[34] Nedoma, A. J.; Robertson, M. L.; Wanakule, N. S.; Balsara, N. P. Measurements of the composition and molecular weight dependence of the Flory-Huggins interaction parameter. *Macromolecules* **2008***, 41*, 5773-5779.

[35] Yang, H., Shibayama, M., Stein, R. S., Shimizu, N. & Hashimoto, T. Deuteration effects on the miscibility and phase separation kinetics of polymer blends. *Macromolecules* **1986**, *19*, 1667–1674.
[36] Russell, T. P.; Fetters, L. J.; Clark, J. C.; Bauer, B. J.; Han, C. C. Concentration Fluctuations in Mixtures of Linear and Star-Shaped Polymers. *Macromolecules* **1990**, *23*, 654-659.
[37] Minnikanti, V. S.; Archer, L. A. Surface migration of branched molecules: Analysis of energetic and entropic factors. *J. Chem. Phys.* **2005**, *123*, 144902.
[38] Minnikanti, V. S.; Archer, L. A. Entropic attraction of polymers toward surfaces and its relationship to surface tension. *Macromolecules* **2006**, *39*, 7718-7728.
[39] Qian, Z.; Minnikanti, V. S.; Sauer, B. B.; Dee, G. T.; Archer, L. A. Surface tension of symmetric star polymer melts. *Macromolecules* **2008**, *41*, 5007-5013.
[40] Taddese, T.; Carbone, P.; Cheung, D. L. Thermodynamics of linear and star polymers at fluid interfaces. *Soft Matter* **2015**, *11*, 81-93.
[41] Striolo, A.; Prausnitz, J. M. Adsorption of branched homopolymers on a solid surface. *J. Chem. Phys.* **2001**, *114*, 8565-8572.
[42] Karim, T. B.; McKenna, G. B. Comparison of surface mechanical properties among linear and star polystyrenes: Surface softening and stiffening at different temperatures. *Polymer* **2013**, *54*, 5928-5935.
[43] Grayce, C. J.; Schweizer, K. S. A Liquid-State Theory of Dense Star Polymer Fluids. *Macromolecules* **1995**, *28*, 7461-7478.
[44] Wu, W.; Wang, W.; Li, J. Star polymers: Advances in biomedical applications. *Progress in Polymer Science* **2015**, *46*, 55-85.
[45] Chremos, A.; Douglas, J. F. Communication: When does a branched polymer become a particle? *J. Chem. Phys.* **2015**, *143*, 111104.
[46] Chremos, A.; Glynos, E.; Green, P. F. Structure and dynamical intra-molecular heterogeneity of star polymer melts above glass transition temperature. *J. Chem. Phys.* **2015**, *142*, 044901.
[47] Frieberg, B.; Glynos, E.; Sakellariou, G.; Green, P. F. Physical Aging of Star-Shaped Macromolecules. *Acs Macro Letters* **2012**, *1*, 636-640.

[48] Glynos, E.; Chremos, A.; Frieberg, B.; Sakellariou, G.; Green, P. F. Wetting of Macromolecules: From Linear Chain to Soft Colloid-Like Behavior. *Macromolecules* **2014**, *47*, 1137-1143.
[49] Glynos, E.; Frieberg, B.; Chremos, A.; Sakellariou, G.; Gidley, D. W.; Green, P. F. Vitrification of Thin Polymer Films: From Linear Chain to Soft Colloid-like Behavior. *Macromolecules* **2015**, *48*, 2305-2312.
[50] Glynos, E.; Frieberg, B.; Green, P. F. Wetting of a Multiarm Star-Shaped Molecule. *Phys. Rev. Lett.* **2011**, *107*, 118303.
[51] Likos, C. N.; Lowen, H.; Watzlawek, M.; Abbas, B.; Jucknischke, O.; Allgaier, J.; Richter, D. Star polymers viewed as ultrasoft colloidal particles. *Phys. Rev. Lett.* **1998**, *80*, 4450-4453.
[52] Pakula, T. Static and dynamic properties of computer simulated melts of multiarm polymer stars. *Computational and Theoretical Polymer Science* **1998**, *8*, 21-30.
[53] Patil, R.; Schweizer, K. S.; Chang, T. M. Stretching, packing, and thermodynamics in highly branched polymer melts. *Macromolecules* **2003**, *36*, 2544-2552.
[54] Vlassopoulos, D. Colloidal star polymers: Models for studying dynamically arrested states in soft matter. *Journal of Polymer Science Part B-Polymer Physics* **2004**, *42*, 2931-2941.
[55] Chremos, A.; Camp, P. J.; Glynos, E.; Koutsos, V. Adsorption of star polymers: computer simulations. *Soft Matter* **2010**, *6*, 1483-1493.
[56] Green, P. F.; Glynos, E.; Frieberg, B. Polymer films of nanoscale thickness: linear chain and star-shaped macromolecular architectures. *Mrs Communications* **2015**, *5*, 423-434.
[57] Cowie, J. M. G.; Arrighi, Valeria *Polymers: Chemistry and Physics of Modern Materials;* CRC Press, Taylor & Francis Group: United States of America, 2008.
[58] Higgins, J. S.; Lipson, J. E. G.; White, R. P. A simple approach to polymer mixture miscibility. *Philosophical Transactions of the Royal Society A-Mathematical Physical and Engineering Sciences* **2010**, *368*, 1009-1025.
[59] White, R. P.; Lipson, J. E. G.; Higgins, J. S. New Correlations in Polymer Blend Miscibility. *Macromolecules* **2012**, *45*, 1076-1084.

[60] White, R. P.; Lipson, J. E. G. Free Volume, Cohesive Energy Density, and Internal Pressure as Predictors of Polymer Miscibility. *Macromolecules* **2014***, 47*, 3959-3968.
[61] White, R. P.; Lipson, J. E. G.; Higgins, J. S. How Pure Components Control Polymer Blend Miscibility. *Macromolecules* **2012***, 45*, 8861-8871.
[62] DeFelice, J.; Lipson, J. E. G. Polymer Miscibility in Supercritical Carbon Dioxide: Free Volume as a Driving Force. *Macromolecules* **2014***, 47*, 5643-5654.
[63] Lipson, J. E. G.; White, R. P. Connecting Theory and Experiment To Understand Miscibility in Polymer and Small Molecule Mixtures. *J. Chem. Eng. Data* **2014***, 59*, 3289-3300.
[64] White, R. P.; Lipson, J. E. G. Chain fluids: Contrasts of theoretical and simulation approaches, and comparison with experimental alkane properties. *J. Chem. Phys.* **2009***, 131*, 074109.
[65] White, R. P.; Lipson, J. E. G. Fluid mixtures: Contrasts of theoretical and simulation approaches, and comparison with experimental alkane properties. *J. Chem. Phys.* **2009***, 131*, 074110.
[66] Lipson, J. E. G. A Born-Green-Yvon Integral-Equation Treatment of Incompressible Lattice Mixtures. *J. Chem. Phys.* **1992***, 96*, 1418-1425.
[67] Guggenheim, E. Statistical thermodynamics of mixtures with zero energies of mixing. *Proceedings of the Royal Society of London Series A-Mathematical and Physical Sciences* **1944***, 183*, 0203-0212.
[68] Graessley, W. W. Polymer Liquids and Networks: Structure and Properties; Garland Science, Taylor and Francis Group: New York, 2004.
[69] Krishnamoorti, R.; Graessley, W.; Dee, G.; Walsh, D.; Fetters, L.; Lohse, D. Pure component properties and mixing behavior in polyolefin blends. *Macromolecules* **1996***, 29*, 367-376.
[70] The dPS samples were kindly provided by Professor Nigel Clark. The *PVT* data were measured by DatapointLabs, Ithaca, NY, using a Gnomix *PVT* apparatus which has an accuracy of 0.002 mL/g (ref 71).
[71] Zoller, P.; Walsh, D. *Standard Pressure-Volume-Temperature Data for Polymers*; Technomic Pub Co.: Lancaster, PA, 1995.

[72] Guo, J.; Grassia, L.; Simon, S. L. Bulk and shear rheology of a symmetric three-arm star polystyrene. *Journal of Polymer Science Part B-Polymer Physics* **2012***, 50*, 1233-1244.
[73] Buckingham, A.; Hentschel, H. Partial Miscibility of Liquid-Mixtures of Protonated and Deuterated High Polymers. *Journal of Polymer Science Part B-Polymer Physics* **1980***, 18*, 853-861.
[74] Beaucage, G.; Stein, R.; Hashimoto, T.; Hasegawa, H. Tacticity Effects on Polymer Blend Miscibility. *Macromolecules* **1991***, 24*, 3443-3448.
[75] Ubrich, J.; Larbi, F.; Halary, J.; Monnerie, L.; Bauer, B.; Han, C. Molecular-Weight Effects on the Phase-Diagram of Polystyrene Polyvinyl Methyl-Ether) Blends. *Macromolecules* **1986***, 19*, 810-815.

for Table of Contents use only

The Effects of Branching and Deuterium Labeling on Blend Miscibility

Jeffrey DeFelice, Julia S. Higgins, and Jane E. G. Lipson